Türk Biyokimya Dergisi [Turkish Journal of Biochemistry–Turk J Biochem] 2009; 34 (3) ; 128–133.

Research Article [Araştırma Makalesi]

Yayın tarihi 25 Eylül, 2009 © TurkJBiochem.com

[Published online 25 September, 2009]

Comparative Study of the Reduction of Phenoxazine and Phenothiazine Dyes by NADH in Aqueous Solution

[Sulu Çözeltide Fenoksazin ve Fenotiyazin Boyaların NADH ile İndirgenmesinin Karşılaştırmalı Çalışması]

Özden Tacal,
İnci Özer

Department of Biochemistry, School of Pharmacy
Hacettepe University 06100 Ankara, Turkey

Yazışma Adresi
[Correspondence Address]

Dr Özden Tacal

Department of Biochemistry, School of Pharmacy
Hacettepe University
06100 Ankara, Turkey
Fax: (90) 312- 4322604
E-mail: tacal@hacettepe.edu.tr

Registered: 16 February 2009; Accepted: 04 May 2009
[Kayıt Tarihi: 16 Şubat 2009; Kabul Tarihi: 04 Mayıs 2009]

ABSTRACT

Objective: To compare the kinetics of the reduction of phenoxazine and phenothiazine dyes by NADH.

Method: The kinetics of the reduction of meldola blue, nile blue, toluidine blue O, methylene blue, thionine by NADH in aqueous solution were studied spectrophotometrically.

Results: The reactions involved intermediate dye-NADH complex formation. In the case of meldola blue and thionine, the formation of the complex was accompanied by a change in dye absorbance, pointing to charge transfer interaction between donor and acceptor species. The reduction of toluidine blue O, methylene blue and Nile blue proceeded without intermediate changes in absorptivity. The turnover rate constants (k) for the dye-NADH complexes were 66 ± 3.0 min^{-1} (for meldola blue), 5.4 ± 1.4 min^{-1} (for thionine), 0.77 ± 0.15 min^{-1} (for toluidine blue O), 0.16 ± 0.03 min^{-1} (for methylene blue) and 0.10 ± 0.02 min^{-1} (for nile blue).

Conclusion: There was a linear correlation between the redox potentials of the dyes and the reduction rate constants. Dye reduction in solution was characterized by up to 94000-fold lower turnover rate constants than reported for electron transfer between NADH and surface-immobilized dyes in electrocatalytic NADH oxidation. Comparison of the redox behavior of free and immobilized dyes suggested that electron transfer on electrode surfaces must be rate-limited by physical phenomena.

Keywords: Charge transfer complex; phenoxazine dyes; phenothiazine dyes; NADH.

ÖZET

Amaç: Fenoksazin ve fenotiyazin boyaların NADH ile indirgenme kinetiklerini karşılaştırmak.

Yöntem: Sulu çözeltide meldola mavisi, nil mavisi, toluidin mavisi O, metilen mavisi, tiyoninin NADH ile indirgenme kinetikleri spektrofotometrik olarak çalışıldı.

Bulgular: Reaksiyonlar esnasında boya-NADH ara kompleks oluşumu meydana geldi. Meldola mavisi ve tiyonin ile yapılan çalışmalarda, verici ve alıcı türler arasındaki yük transfer etkileşimi olduğunu işaret eden boya absorbansındaki bir değişiklik, kompleks oluşumuna eşlik etti. Toluidin mavisi, metilen mavisi ve nil mavisinin indirgenmesi, absorptivitede değişiklikler olmadan ilerledi. Boya-NADH kompleksleri, için devretme hız sabitleri (k) 66 ± 3.0 dak-1 (for meldola mavisi için), 5.4 ± 1.4 dak-1 (tiyonin için), 0.77 ± 0.15 min-1 (toluidin mavisi O için), 0.16 ± 0.03 dak-1 (metilen mavisi için) ve 0.10 ± 0.02 dak-1 (Nil mavisi için) bulundu.

Sonuç: Boyaların redoks potansiyelleri ile indirgenme hız sabitleri arasında bir lineer ilişki vardı. Çözeltide boyanın indirgenmesi, elektrokatalitik NADH oksidasyonunda yüzey immobilize boya ve NADH arasındaki elektron transferi için bildirilen devretme hız sabitinden 94000 kata kadar daha düşük bulundu. Serbest ve immobilize boyaların redoks davranışının karşılaştırılması, elektrot yüzeyinde elektron transfer hızını kısıtlayıcı faktörün fiziksel olması gerektiğini gösterdi.

Anahtar kelimeler: Yük transfer kompleksi; fenoksazin boyalar; fenotiyazin boyalar; NADH.

Introduction

Studies on the catalytic effect of phenoxazine and phenothiazine dyes on the electrochemical oxidation of NAD(P)H (a common primary or indicator analyte in biosensors [1-7]) have shown electron flow from the reduced cofactors to the redox mediators to be a nonlinear function of cofactor concentration, implicating the intermediate formation of an NAD(P)H*dye charge transfer complex at the electrode interface [1-5,8,9]. Charge transfer (CT) complexes between nicotinamide cofactors and quinoid redox centers have also been shown to form in the catalytic cycle of NADPH-dependent flavoenzymes and in intramolecular hydride transfer in a covalently linked model system (flavin-nicotinamide biscoenzyme) in solution [10-13]. Our recent study on the inhibition of choline oxidase by a number of quinoid dyes including meldola blue (MB), nile blue (NB) and methylene blue (MetB) likewise pointed to likely CT-type interactions between the dyes and the flavin prosthetic group [14]. In search of basic information on the redox behavior of simpler systems involving free donor and acceptor species in solution, we now report on the reactions of NADH with 5 dyes having a phenoxazine or phenothiazine nucleus (Figure 1). The results are consistent with electron transfer via complex formation and offer clues relating to the kinetic performance of electrochemical systems and development of electrodes for bioanalytical applications.

Materials and Methods

Materials and reagents

MB zinc chloride salt, NB chloride, thionine (TH) acetate, toluidine blue O (TBO) and β-nicotinamide adenine dinucleotide (NADH) were purchased from Sigma-Aldrich Chemical Co., USA. MetB was obtained from Merck, Germany. Stock solutions of the dyes (5 mM, based on nominal dye content) were prepared daily in methanol. Solutions of NADH in distilled water were prepared just before use.

Kinetic Measurements

The redox reactions were carried out at 25°C in a Shimadzu 1601 PC spectrophotometer equipped with a Peltier unit. The reaction mixture consisted of 50 mM 3-(N-morpholino)propanesulfonic acid (MOPS) buffer (pH 7), 0-2 mM NADH and 0-100 μM dye. The process was initiated by the addition of dye and monitored through the decrease in A_{340} (l = 0.5 cm; $\varepsilon_{340,NADH}$ = 6.22 $mM^{-1}cm^{-1}$).

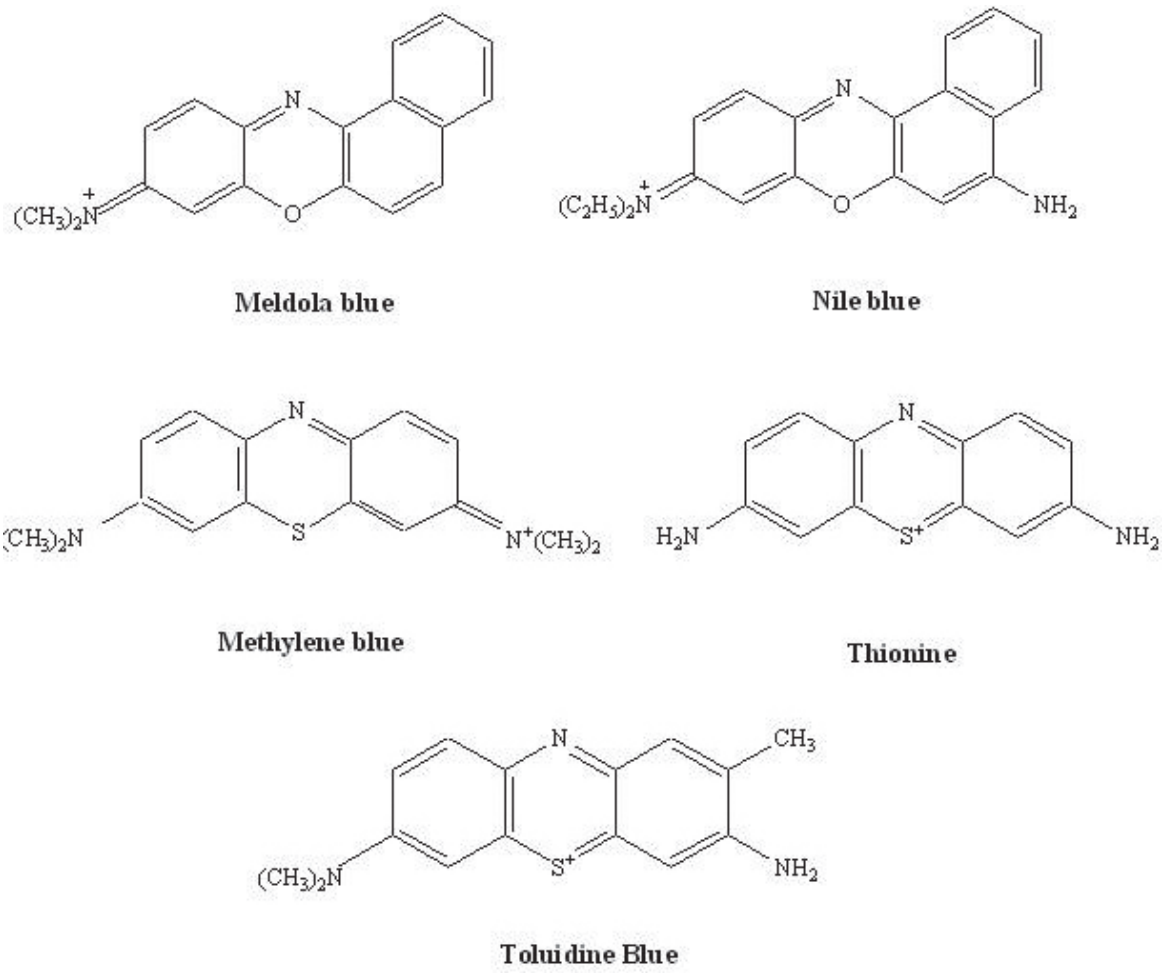

Figure 1. The structure of the dyes studied.

Where applicable, the change in absorbance at the λ_{max} of the dye was also monitored.

Results

The Reaction of NADH with MB and TH

The reaction of MB with NADH, monitored at 570 nm, traced a biphasic course (Figure 2A), which involved rapid loss in dye absorbance (Phase I), followed by a slow recovery to ca. 90% of the zero-time value (Phase II). The corresponding profile for NADH exhibited an initial incremental drop in A_{340}, followed by steady turnover to NAD^+ (Figure 2B). The progress curves were evaluated on the basis of Scheme I, where hydride transfer is preceded by the formation of a charge transfer complex, MB*NADH. (The scheme is similar to the one proposed in connection with the electrocatalytic oxidation of nicotinamide cofactors [1], except for the substitution of molecular oxygen as the terminal electron acceptor).

$$MB^+ + NADH \underset{K_d}{\overset{}{\rightleftharpoons}} MB^*NADH \xrightarrow{k} MBH + NAD^+$$

$$k_{O2}[O_2]$$

SCHEME I.

The shape and duration of Phase I in the A_{570} *vs* t curve suggested that the rapid initial decrease in absorbance was the combined result of complex formation and reduction of initially available MB and that Phase II reflected the balance between O_2-mediated regeneration and NADH-mediated redepletion of the dye. The high rates of complex formation and reduction precluded rigorous quantitation of K_d and k in Scheme I by standard kinetic monitoring. However, since O_2-mediated regeneration was obviously rate-limiting ($k_{O2}[O_2] = k_{O2}' \approx 0.06$ sec^{-1}, as determined from the latter half of Phase II in Fig. 2A) estimates for the two parameters were made by assuming that complex formation is immeasurably fast and that the tail of Phase I in the A_{570} profile reflects the "first-pass" conversion of MB*NADH to MBH + NAD^+. The process is governed by Equation 1a

$$-dA_{570}/dt = k\,[MB^*NADH]_t \qquad (1a)$$

and may be analyzed by Eqs 1b-1d, provided $[NADH]_o >> [MB]_o$ [15],

$$-dA_{570}/dt \approx k\,[MB]_t\,[NADH]_o / (K_d + [NADH]_o) \qquad (1b)$$

$$\approx k'\,[MB]_t \qquad (1c)$$

which integrates to

$$\ln (A_t - A_\infty) = \ln (A_o - A_\infty) - k't \qquad (1d)$$

Semilogarithmic plots of $(A_t - A_\infty)$ relating to Phase I *versus* time were linear, bearing out the assumption made (Figure 3A). Referring to the relationship, k' = k

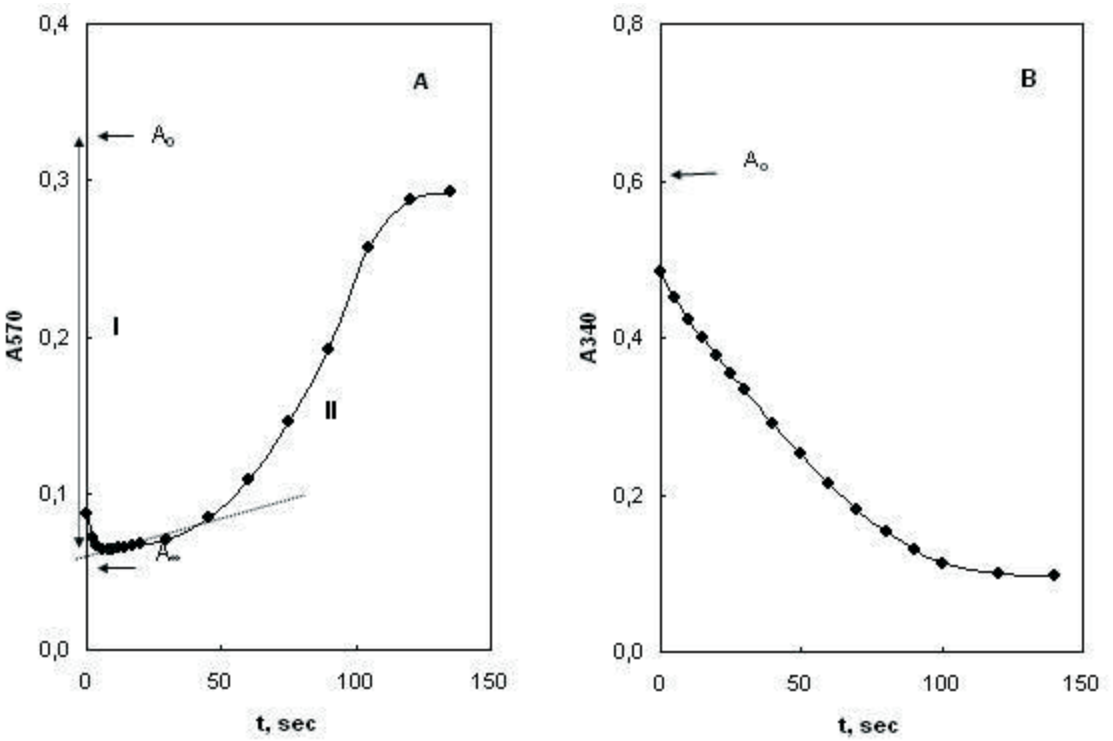

Figure 2. Progress curves for the reaction of NADH with meldola blue. Variation in the levels of cationic dye (A) and NADH (B). $[MB^+]_o$ = 50 µM; $[NADH]_o$ = 170 µM (pathlength, 0.5 cm). A_∞ marks the end-point value for Phase I (see text).

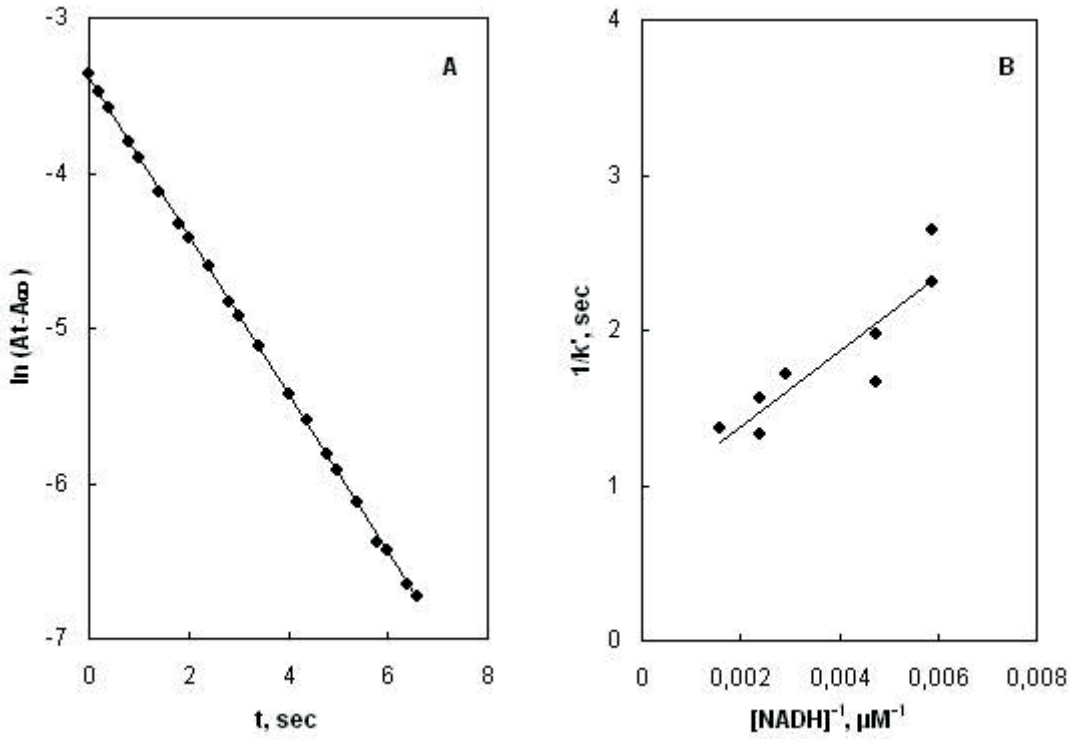

Figure 3. (A) Semilogarithmic plot of the change in MB absorbance in Phase I as a function of time. [MB] = 30 µM; [NADH] = 210 µM. (B) The dependence of the observed rate constant for dye reduction on NADH concentration. [MB] = 30 µM.

$[NADH]_o$ / (K_d + $[NADH]_o$), a double reciprocal plot of k' *vs* $[NADH]_o$ (Figure 3B) yielded K_d = 0.27 ± 0.040 mM and k = 66 ± 3.0 min^{-1}

The reduction of thionine by NADH proceeded more slowly and yielded a better resolved absorbance-time profile which conformed to Scheme I (Figure 4): An initial fast drop in A_{599} (Phase I, charge transfer complex formation) was succeded by a measurably slow reduction step (Phase II, dye reduction) and a steady-state determined by the relative rates of reduction and air-oxidation (Phase III). K_d for the TH*NADH complex was determined by processing the amplitude of the change in dye absorbance in Phase I (λ = 599 nm) according to Eq. 2 and was found to be 2.0 ± 0.45 mM.

$$K_d = \frac{[TH]_{free}[NADH]_{free}}{[TH*NADH]} \qquad (2)$$

($[TH]_{free}$ = $[TH]_o A_{o,II}/A_o$; A_o = A_{599} in the absence of NADH; $A_{o,II}$ = A_o in the presence of NADH, marking the starting point of Phase II (cf Fig 4A); [TH*NADH] = $[TH]_o$ – $[TH]_{free}$; $[NADH]_{free}$ = $[NADH]_o$ – [TH*NADH]). The turnover rate constant (k) was estimated by using the initial rates of change in A_{340} *in the first 60-sec segment of Phase II* (Fig. 4B) and the relationship, $(-dA_{340}/dt)_i$ = k $[TH*NADH]_i$. ([TH*NADH] was calculated as described above). At 50 µM TH/85-510 µM NADH and 15-100 µM TH/170 µM NADH, k averaged 5.4 ± 1.4 min^{-1}.

The Reactions of NADH with TBO, MetB and NB

Due to the immediate O_2-mediated reoxidation of the reduced dye species, the reduction of TBO, MetB and NB by NADH could not be monitored through changes in dye absorbance. There were also no transient changes in dye or NADH absorbance to implicate charge transfer complex formation. The presence of a dye*NADH complex on the reaction pathway and the conformity of the system to Scheme I could only be tested by studying the concentration dependence of the initial rates of NADH depletion as reflected in A_{340}: Scheme I (with $k_{O2}[O_2] >> k$) and Equations 3 a-c (analogous to Eqs 1 a-c used to describe dye depletion) predict a hyperbolic relationship between v_i and $[NADH]_o$.

$$v_i = (-d[NADH]/dt)_i = k\,[dye*NADH]_i \qquad (3a)$$
$$= k\,[dye]_o\,[NADH]_o/(K_d + [NADH]_o \qquad (3b)$$
$$= k'\,[NADH]_o/(K_d + [NADH]_o) \qquad (3c)$$

Diagnostic double reciprocal plots of v_i^{-1} *vs* $[NADH]_o^{-1}$ were linear and had non-zero ordinate intercepts, validating the multi-step nature of the redox process (Figure 5). The reaction parameters (K_d and k) were estimated according to Eq. 3d.

$$\frac{1}{v_i} = \frac{K_d}{k'\,[NADH]_o} + \frac{1}{k'} \qquad (3d)$$

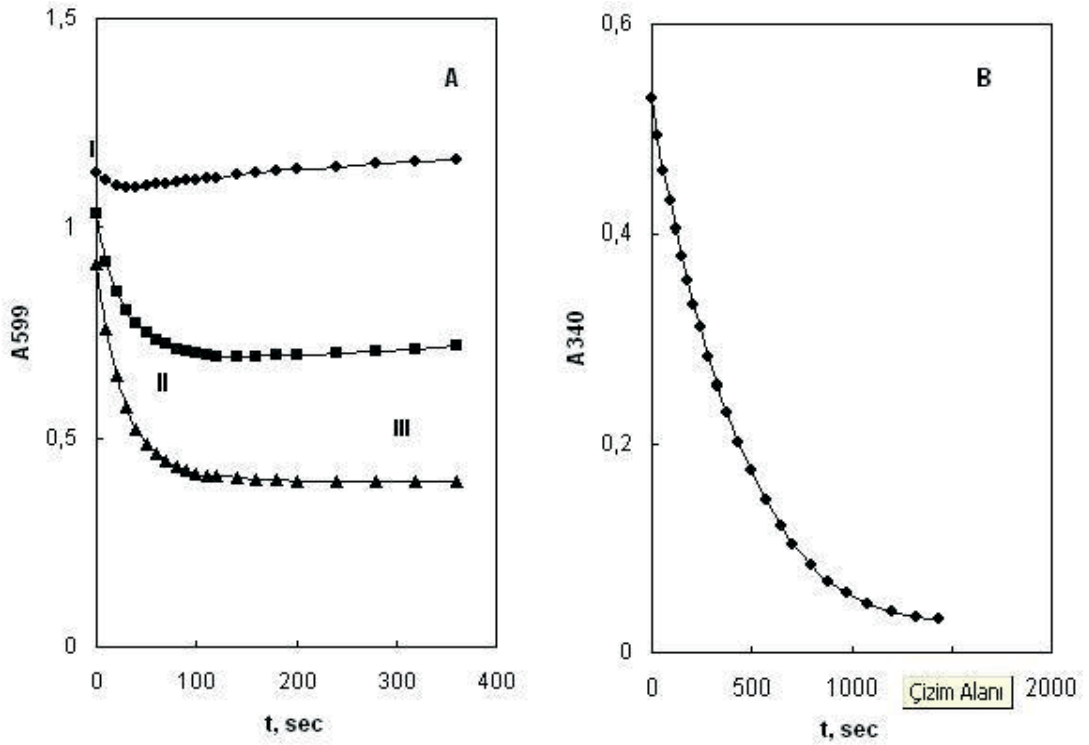

Figure 4. Progress curves for the reaction of NADH with thionine. (A) Depletion of cationic dye at (♦)170, (■) 340 and (▲) 510 μM NADH. [TH] = 50 μM. (B) Depletion of 170 μM NADH at 50 μM TH. (Pathlength, 0.5 cm).

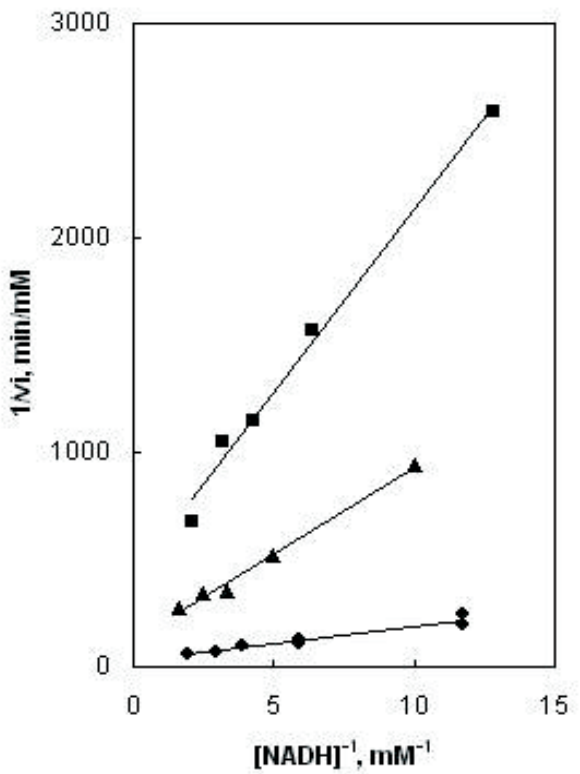

Figure 5. Double reciprocal plots of the initial rate of NADH depletion at 50 μM TBO (●), 15 μM MetB (■) and 50 μM NB (▲).

K_d and k values for TBO, MetB and NB were 0.63 ± 0.18 mM, 0.77 ± 0.15 min^{-1}; 0.42 ± 0.05 mM, 0.16 ± 0.03 min^{-1}; 0.52 ± 0.08 mM, 0.10 ± 0.015 min^{-1}, respectively.

Discussion

The reaction of NADH with phenoxazine/phenothiazine dyes in aqueous solution was found to proceed through a dye*NADH complex. The K_d values for the complex failed to reveal a specific pattern and fell in the 0.27-2.0 mM range. These values compare favorably with those reported in connection with the electrocatalytic oxidation of NADH by surface immobilized dyes (K_d = 0.15-1.1 mM) [2, 4, 8, 9, 16-18].

In contrast to the K_d values, the rate constants for the reactions in solution displayed an overall positive relationship with the E_o' value of the dye as acceptor. The reductions of MB, TH, TBO and MetB revealed a strictly linear relationship between log k and E_o' (Figure 6, filled symbols; r^2 = 0.992). Evaluated within the linear free energy framework set by the 4 dyes, NB appeared to be 250-fold more reactive than expected. The reason for this hyperreactivity is not immediately obvious. A survey of reports dealing with the behavior of NADH-dye couples in electrocatalytic systems shows that the k-E_o' relationship observed with the dyes in aqueous solution is lacking in such systems (Fig. 6, open symbols): The electrochemical k values show considerable scatter around a zero-slope trendline, converging with the fam-

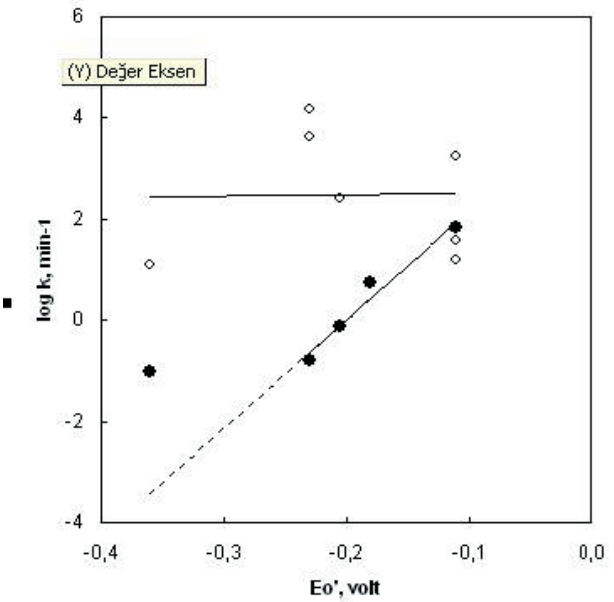

Figure 6. Free energy relationships in electron transfer between NADH and phenoxazine/phenothiazine dyes.

Filled symbols: k values for MB (E_o', -0.110 V [17]), TH (E_o', -0.180 V [4])), TBO (E_o', -0.210 V [4, 17]), MetB (E_o', -0.230 V [4])) and NB (E_o', -0.360 V [17]) in solution.

Open symbols: Electrochemical k values compiled from [2, 8,9,16,17].

ily of k values obtained in the present study at the point corresponding to MB in solution. This suggests that rate constants observed in electrochemical systems reflect not the process of electron transfer between donor and acceptor, but an interfacial process. Such a physical factor could also explain the wide range of k values reported for MB (15-1800 min^{-1} [2, 16]) and highlight the electrode surface as a primary determinant in redox devices. These results show that formation of charge transfer complex occurs in aqueous solutions (therefore in vivo) and development of biological effects of these dyes partially depend on deterioration of redox equilibrium and processes. Therefore, this work may help development of electrodes for bioanalytical applications.

Acknowledgement

This study has been supported by a grant (SBAG-2912) from the Scientific and Technical Research Council of Turkey.

References

[1] Gorton L, Torstensson A, Jaegfeldt H, Johansson G. (1984) Electrocatalytic oxidation of reduced nicotinamide coenzymes by graphite electrodes modified with an adsorbed phenoxazinium salt, meldola blue. J. Electroanal. Chem. 161 (1): 103-120.

[2] Gorton L. (1986) Chemically modified electrodes for the catalytic oxidation of nicotinamide coenzymes. J. Chem. Soc. Faraday Trans I 82 (4): 1245-1258.

[3] Chi Q, Dong S. (1995) Electrocatalytic oxidation of reduced nicotinamide coenzymes at organic dye-modified electrodes. Electroanal. 7 (2): 147-153.

[4] Kubota LT, Gorton L. (1999) Electrochemical study of flavins, phenazines, phenoxazines and phenothiazines immobilized on zirconium phosphate. Electroanal. 11 (10-11): 719-728.

[5] Lobo MJ, Miranda AJ, Tunon P. (1997) Amperometric biosensors based on NAD(P)-dependent dehydrogenase enzymes. Electroanal. 9 (3): 191-202.

[6] Lobo MJ, Miranda AJ, Tunon P. (1996) A comparative study of some phenoxazine and phenothiazine modified carbon paste electrodes for ethanol determination. Electroanal. 8 (6): 591-596.

[7] Forrow NJ, Sanghera GS, Walters SJ, Watkin JL. (2005) Development of a commercial amperometric biosensor electrode for the ketone D-3-hydroxybutyrate. Biosens Bioelectron. 20 (8): 1617-1625.

[8] Santos AD, Gorton L, Kubota LT. (2002) Nile blue adsorbed onto silica gel modified with niobium oxide for electrocatalytic oxidation of NADH. Electrochim. Acta 47 (20): 3351-3360.

[9] Komura T, Niu GY, Yamaguchi T, Asano M, Matsuda A. (2004) Coupled electron-proton transport in electropolymerized methylene blue and the influence of its protonation level on the rate of electron exchange with beta-nicotinamide adenine dinucleotide. Electroanal. 16 (21): 1791-1800.

[10] Blankenhorn G. (1975) Flavin-nicotinamide biscoenzymes: models for the interaction between NADH (NADPH) and flavin in flavoenzymes. Eur J Biochem. 50 (2): 351-356.

[11] Danielson UH, Jiang F, Hansson LO, Mannervik B. (1999) Probing the kinetic mechanism and coenzyme specificity of glutathione reductase from cyanobacterium anabaena PCC7120 by redesign of the pyridine nucleotide binding site. Biochemistry 38 (29): 9254-9263.

[12] Knight K, Scrutton NS. (2002) Stopped-flow kinetic studies of electron transfer in the reductase domain of neuronal nitric oxide synthase: reevaluation of the kinetic mechanism reveals new enzyme intermediates and variation with cytochrome P450 reductase. Biochem J. 367: 19-30.

[13] Wolthers KR, Scrutton NS. (2004) Electron transfer in human methionine synthase reductase studied by stopped-flow spectrophotometry. Biochemistry 43 (2): 490-500.

[14] Tacal Ö, Özer I. (2006) Inhibition of choline oxidase by quinoid dyes. J Enz Inhib Med Chem. 21 (6): 783-787.

[15] Özer I. (2005) Reactivity of meldola blue towards sulfydryl groups: Analytical and biomedical aspects. Turk J Biochem 30 (3): 220-224.

[16] Santos AD, Gorton L, Kubota LT. (2002) Electrocatalytic NADH oxidation using electrode based on meldola blue immobilized on silica coated with niobium oxide. Electroanal. 14 (12): 805-812.

[17] Cai CX, Xue KH. (2000) The effects of concentration and solution pH on the kinetic parameters for the electrocatalytic oxidation of dihydronicotinamide adenine dinucleotide (NADH) at glassy carbon electrode modified with electropolymerized film of toluidine blue O. Microchem J. 64 (2): 131-139.

[18] Persson B, Gorton L. (1990) A comparative study of some 3, 7-diaminophenoxazine derivatives and related compounds for electrocatalytic oxidation of NADH. J Electroanal Chem. 292 (1-2): 115-138.